Flame front tracking and simultaneous flow field visualization in turbulent combustion

by

J. Hult[1], G. Josefsson[2], M. Aldén[1] and C.F. Kaminski[1]

[1]Lund Institute of Technology
Division of Combustion Physics
Box 118, S-22100 Lund, Sweden
Fax: +46 (0)46 2224542
E-mail: johan.hult@forbrf.lth.se

[2]Volvo Technological Development Corporation
Dept. 6110, PVOA 201
S-40508 Göteborg, Sweden
Fax: +46 (0)31 546710
E-mail: gojo@vtd.volvo.se

ABSTRACT

Local extinction phenomena have a major influence on flame stability and a better understanding of the mechanisms leading to extinction is both of fundamental and practical importance. To study the importance of large scale structures for local flame extinction two-dimensional measurements of relevant quantities with high time resolution are desirable. Simultaneous measurements of both flow and flame quantities, allowing correlations between the two to be studied, are also useful in this respect. The present paper reports on a novel measurement technique which allows simultaneous time resolved measurements of the evolution of the OH radical distribution and the instantaneous velocity field in turbulent flames to be made. The combined measurement technique can be used to study the dynamics of turbulence/chemistry interactions in real time. High speed planar laser induced fluorescence (PLIF) of OH at repetition rates exceeding 13 kHz was used to track the response of the flame front to the turbulent flow field. From the OH PLIF sequences the position, in both space and time, where the local extinction of the flame front begins, could be identified. The temporal changes in local OH distribution during the extinction process could also be studied and the time scale of extinction events estimated. For the PLIF measurements a multiple Nd:YAG laser cluster and a high speed camera, consisting of several CCD units, were used. Instantaneous velocity field measurements were performed simultaneously using particle image velocimetry (PIV). In the velocity field the flow structures associated with the identified extinction events were visualized. The object of study was the TECFLAM turbulent non-premixed flame which serves as an international standard for model validation. Vortices impinging from the fuel side on the flame front was the dominating extinction mechanism found. Sequences recorded at various heights illustrating this mechanism are presented.
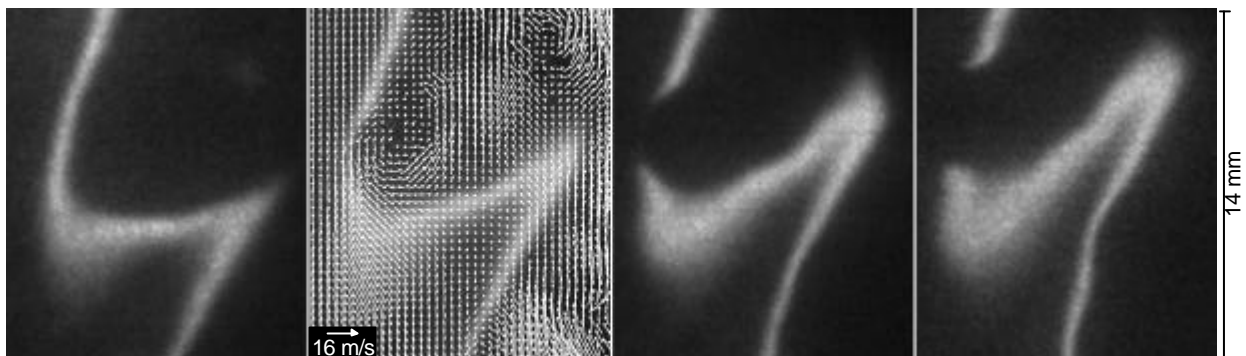
Figure 0: Sequence of OH distributions in the TECFLAM turbulent non-premixed flame, Re≈20000. The time separation between consecutive images is 125 ms. The flow field was measured simultaneously with the second OH concentration image, and is plotted on top of this image In the PIV image a mean vertical velocity of 9 m/s has been subtracted from the velocity vectors. A local extinction phenomenon is shown at a position 19 nozzle diameters above the burner; a vortex from the fuel side (to the right) impinges on the flame front and extinguishes the flame front.

1. INTRODUCTION

Understanding of the stability of turbulent non-premixed flames is both of fundamental and practical importance because of their widespread appearance in combustion applications. One of the phenomena of major influence on flame stability and combustion efficiency is extinction. Strong interaction between turbulence and chemistry taking place near the flame front can lead to local extinction. Flame-vortex interactions (FVI) leading to local extinction have been studied numerically using direct numerical simulation (DNS) (Cuenot and Poinsot, 1994 and Takahashi and Katta., 1996) and computational fluid dynamics with chemistry (CFDC) (Katta et al., 1998).

To increase the understanding of turbulence-chemistry interaction phenomena such as local flame extinction further experimental studies performed in fully turbulent flames are needed. These experiments should provide two-dimensional (2-D), or ideally three-dimensional (3-D), measurement data of large scale structures which are believed to play an important role. As the process is inherently time-dependent these experiments should be performed with high time resolution to reveal the dynamics of the events. Finally, simultaneous measurements of several quantities allow correlations between various flow and flame quantities to be studied. Studies focusing on local extinction phenomena in turbulent non-premixed flames which have fulfilled some of these criteria, have been reported in the past (Stårner et al., 1992, Takahashi and Goss, 1992, Schefer et al., 1994, Takahashi et al., 1996, Rehm and Clemens, 1998 and Watson et al., 1999).

For 2-D studies of turbulent reacting flows laser based diagnostic techniques are especially useful (Hanson, 1986). Instantaneous 2-D measurements of species concentrations using planar laser induced fluorescence (PLIF) (Aldén et al., 1982) and of flow fields using particle image velocimetry (PIV) (Raffel et al., 1998) have been used to characterize reactive flows statistically. These instantaneous measurement techniques can easily be extended to time resolved techniques by phase locking the experimental system to reproducible events, such as flame-vortex interactions leading to local extinction in laminar non-premixed flames, and by collecting data at different phase positions (Mueller and Schefer, 1998 and Katta et al., 1998). In order to capture the time evolution of a fully turbulent flame however, several laser pulses have to be fired sequentially within a short time interval, as demonstrated using PIV (Oakley et al., 1996), and PLIF (Kychakoff et al., 1987, Atakan et al., 1993, Schefer et al., 1994 and Seizmann et al., 1994). By combing two laser systems simultaneous 2-D measurements of instantaneous scalar and velocity fields, using PIV and PLIF, have been demonstrated in turbulent flames (Stårner et al., 1992, Rehm and Clemens, 1998 and Watson et al., 1999).

This paper reports the first time resolved recordings of flame extinction events using OH PLIF to which simultaneously obtained velocity field data is coupled. The technique was demonstrated in the TECFLAM turbulent non-premixed flame, which serves as international standard for model validation (Bergmann et al., 1998). The high repetition rate OH PLIF sequences, resolved at rates in excess of 13 kHz, show the time evolution of the local OH distribution. The OH radical is an intermediate species produced in the reaction zone, and removed by intermediate three-body recombination reactions. Thus OH can be used as an approximate marker of the instantaneous reaction zone, of which it marks the fuel lean side where the chemical reactions are completed (Watson et al., 1999). It has also been shown that the OH concentration follows the same trend as heat release rate with increasing strain, but at a retarded rate (Rehm and Clemens, 1998). In this study the OH PLIF images were used to study how the reaction zone structure was affected by the turbulent flow field and specifically to locate the extinction phenomena in time and space. The sequences show the evolution of the local OH distribution during extinction and gives an estimate of the time scale of these events. The PIV measurements corresponded to the instantaneous velocity field for one of the images in the OH PLIF sequence. From this velocity field the turbulent structures associated with the local extinction event could be identified.

2. EXPERIMENTAL

2.1 Burner

The flame used in this study was one of the TECFLAM turbulent non-premixed flames that has been subject to previous experimental and computational investigations within the "International Workshop on Measurement and Computation of Turbulent Nonpremixed Flames" (Bergmann et al., 1998). The flame was stabilized on the coflow burner illustrated in figure 2. It consisted of an 8 mm inner diameter tube with a thinned rim at the exit, surrounded by a concentric contoured nozzle
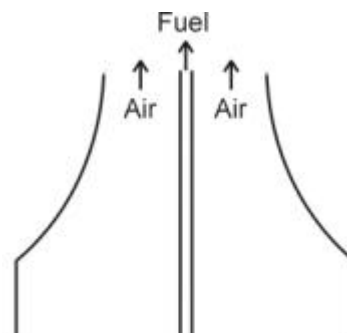

Figure 2: Schematic diagram of the TECFLAM burner used in this study.

with an inner diameter of 140 mm. A mixture of H_2 (33.2% by volume), CH_4 (22.1%) and N_2 (44.7%) was used as fuel, the exit velocity of the fuel jet was 55 m/s, corresponding to a Reynolds number around 20000. The surrounding coflow of air had an exit velocity of 0.3 m/s. Both fuel flow and coflow were seeded with 1 μm titanium (TiO_2) particles gathered from one TSI fluidized bed seeder (fuel flow) and one cyclone seeder (coflow).

2.2 OH PLIF system

For the OH PLIF measurements a high speed laser and detector system was used, which has previously been described in the context of turbulent non-premixed flame studies (Kaminski et al., 1999 and Ding et al., 2000). The laser source was a Nd:YAG laser cluster (BMI, France), consisting of four individual laser heads. Special beam combination optics were used to combine the beams from the four lasers into one beam with minimal associated energy losses. By firing the individual lasers in series a very fast burst of four laser pulses could be obtained, with time separations varying from ~5 ns up to 100 ms between consecutive pulses, the overall repetition rate between consecutive bursts was 10 Hz. In the beam combining process the output was frequency doubled to 532 nm, with a resulting output energy of 450 mJ per pulse.

A commercial tunable dye laser (Continuum) operating on Rhodamine 590 dye was pumped by the pulse train from the Nd:YAG laser cluster. The dye laser output was frequency doubled using a single KdP crystal. During a fast burst of laser pulses the performance of the dye laser pulses was sequentially degraded. The output energy and beam profile quality decreased with decreasing time separation between laser pulses, as there was not enough time to exchange all dye solution in the cuvettes between successive pulses. The decaying output energies for consecutive pulses in a burst could be compensated for by decreasing the energy of the first pumping pulses from the Nd:YAG lasers. This procedure gave output pulses of equal energy, however the energy per pulse was decreased compared to single pulse operation. At a pulse separation of 75 μs an output at 283 nm of 7.5 mJ per pulse could be obtained. To compensate for shot-to-shot laser profile fluctuations an on-line laser profile measurement was performed.

The PLIF detector was a high speed framing camera based on eight individual CCD cameras (Imacon 468, DLR Hadland, UK). Signals were collected via a common optical input and split into eight identical copies, which were relayed to the individual cameras (of which only 4 were used in the present study). Each channel consists of an intensified 8 bit CCD, of 576×385 pixels. By using short exposure times and by exposing the eight cameras in series an image sequence could be captured with high time resolution, down to 10 ns. To increase the light level sensitivity and also to make the camera UV sensitive an additional image intensifier was attached at the optical input. This intensifier which was gated sequentially increased the minimum time separation between images to 1 μs.

OH was excited using the $Q_1(8)$ transition near 283 nm in the $v''=0$, $v'=1$ band of the $A^2\Sigma^+ \leftarrow X^2\Pi$ system. The detected OH fluorescence corresponded to emission in the (1,1) and (0,0) bands near 309 nm.

2.3 PIV system

The light from two Nd:YAG lasers (Spectra-Physics PIV400) was combined and frequency doubled to generate two green light pulses at 532 nm, with a pulse energy of around 250 mJ each. The temporal separation of the two pulses was adjusted to give an optimal signal depending on the velocity of the flow (typically around 10μs). Mie scattering signals from the seeded TiO_2 particles were detected using a 1018×1008 pixel CCD camera (Kodak Megaplus ES1.0). The scattered light was registered as two individual images by the single CCD camera, which was of frame transfer type. The 2-D flow field could be deduced from each pair of PIV images applying a cross correlation technique, using a Dantec PIV2000 processor and Dantec FlowManager software (Dantec Measurement Technology A/S). The system has previously been used for stationary flame studies (Klingmann et al., 1997) and for internal combustion studies (Engström et al., 1999).

2.4 Experimental set-up

A schematic representation of the experimental set-up for the simultaneous OH-PLIF/PIV measurements is shown in figure 3. The frequency doubled OH PLIF beam from the dye laser passed through a f=-40 mm cylindrical lens and a f=+500 mm spherical lens to form a laser sheet approximately 50 mm in height and 0.25

mm in thickness. The OH PLIF signal was detected at right angles using the high speed camera equipped with a UV achromatic lens (Bernhard Halle, f=100 mm, f/2). A long-pass filter (T=50% at λ=295 nm, Laseroptik), was used in combination with a UG 11 filter to reject scattered laser light. A cell filled with fluorescing dye solution and two quartz plates were used to perform the on-line beam profile measurement described above. The first quartz plate reflected about 4% of the laser sheet intensity into the dye solution. PLIF from the dye was reflected by the second quartz plate onto the high speed camera occupying about one fifth of the chip width near the edge of the CCD. In this way the beam profile information was available simultaneously with the OH PLIF image. Linearity of the dye and OH PLIF signals at the intensities used was carefully checked.

A sheet optics module was used to create the PIV laser sheet and to direct it into the flame, coming from the opposite direction to the PLIF sheet. The thickness of the PIV light sheet was approximately 0.4 mm. The PIV camera was positioned in a direction normal to the laser sheets, and on the opposite side of the burner to the PLIF camera. A bandpass filter transmitting only the scattered laser light was mounted on the lens.
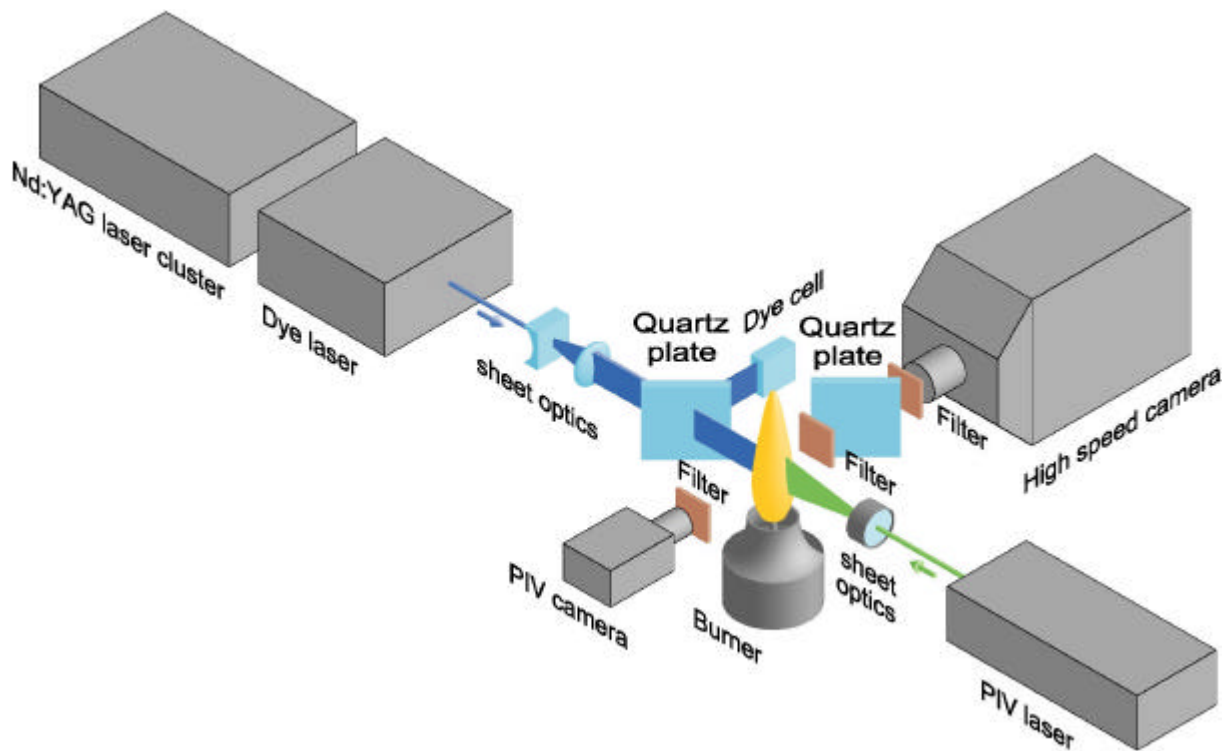

Figure 3: Experimental set-up used for the simultaneous measurements of time-resolved OH concentration and flow field. The OH PLIF system is shown to the upper left and the PIV system is shown to the lower right.

A function generator was used as the master trigger for both laser systems. Every 10 seconds it triggered the Dantec PIV2000 processor, which administered pulses for the PIV laser running continuously at 10Hz. The processor also triggered the Nd:YAG-laser cluster. Individual delays in the two laser systems were then used to fire the PLIF and PIV laser pulses in the correct order. The PLIF high speed camera was triggered by the Nd:YAG laser cluster. The first PIV image was acquired starting 10 µs after the second PLIF image in each sequence. The second PIV image followed another 10 µs later. Two different time separations were used for the OH PLIF sequences, 75 µs in the lower regions of the flame and 125 µs in the higher regions.

In order to change the measurement region in the flame the burner could be translated in radial and axial directions. Measurements were performed in one side of the flame centered on the flame front, at heights ranging from 10 mm to 190 mm above the burner nozzle. The imaged region corresponded to approximately 20×20 mm.

2.5 Data post-processing

The OH PLIF images were corrected for relative image displacements between the individual CCD units in the high speed camera. This was done using geometric transformations (Sonka et al. 1993), which mapped the

individual images to a common reference co-ordinate system. The images were then divided by the recorded laser intensity profiles to compensate for the laser profile fluctuations. As the LIF images were not corrected for quenching, the thermal distribution among energy levels, and saturation effects, the color scale in the resulting images represents pure fluorescence intensity, and does not directly correspond to OH concentration. Thus it mainly gives structural information and only qualitative concentration results.

The PIV images were divided into interrogation areas of 32×32 pixels corresponding to volumes of 0.7×0.7×0.4 mm^3. 62×62 velocity vectors were produced with a 50% overlap between regions giving a spatial vector resolution of 0.35 mm. The instantaneous vector maps were processed using a validation chain that removed erroneous vectors. There are often some erroneous vectors in the raw instantaneous velocity fields and in order to reduce the error a validation process was performed. First a maximum velocity *range validation* was specified which removed all vectors longer than the specified velocity. Then a *peak validation* was made which compared the strongest and the second strongest peak in the cross-correlation evaluation. A criterion on the shape and height of the strongest peak was applied and outliers were removed. As the focus in this work has been on a few vector maps a *manual validation* was applied to remove the obviously erroneous vectors that slipped through the earlier validation schemes. Then a *moving average* comparison was applied where each vector was compared to its neighbours and if it differed too much from the others it was replaced with an interpolated one. This was however very carefully made in order not to create a false velocity pattern. The maximum number of replaced vectors were typically below 10%. When only a few isolated vectors were removed, interpolated vectors were created in the holes of the earlier validations. This 4-step validation chain was individually set for each measurement point and gave the instantaneous vector plots. In the end a subtraction of the mean velocity was made to better visualize the vortex structures in the flow. In the resulting image the air flow to the left is always pointing downwards since the surrounding air flow velocity was lower than both the fuel flow velocity and the average velocity in the flame front region.

Finally the OH images were remapped to the co-ordinate system of the PIV images, again using geometric transformations, and the velocity vectors were plotted on top of the corresponding OH image.

3. RESULTS & DISCUSSION

From the 40-60 image sequences recorded at each height in the flame the sequences where local extinction occurs were identified. These were frequently occurring in the lower regions of the flame, approximately 45 % of the sequences at 10-30 mm above the burner showed at least one local extinction phenomenon, whereas they decreased in number with increasing height over the burner where the larger scale coherent structures were less pronounced. At the highest position studied, 170-190 mm above the burner, only 15 % of the sequences showed local extinction. A number of sequences, taken at different heights, capturing the dynamics of extinction, i.e. showing a closed flame front in the first OH PLIF image and then displaying the break up process, were chosen. A sequence showing re-ignition of an already extinct flame front is also presented. In all image sequences shown the fuel flow is on the right side of the flame front and the air flow is on the left side.
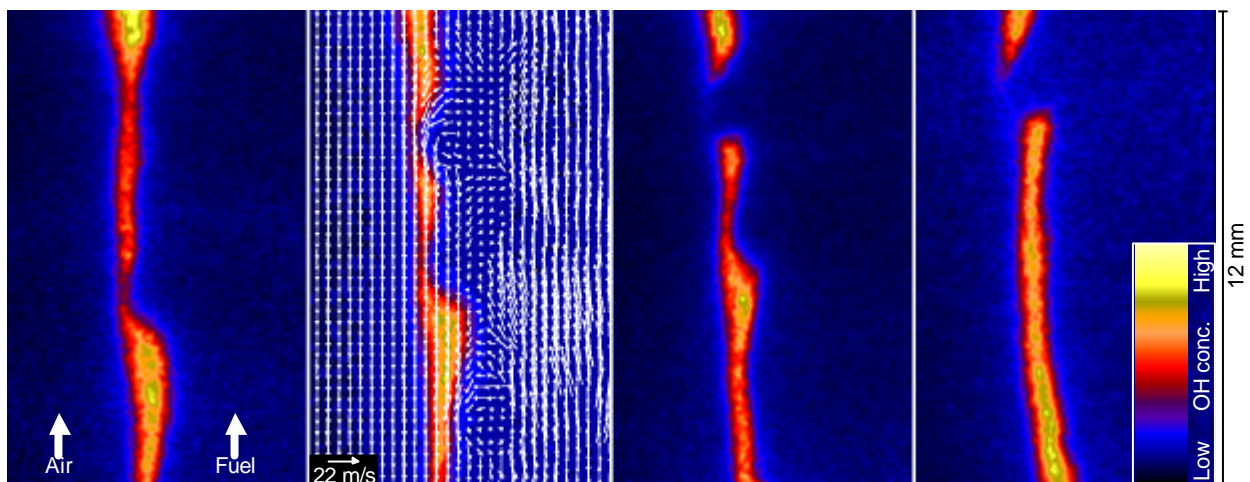

Figure 4: Simultaneous OH PLIF time sequence and velocity field showing a local extinction phenomenon in the lower part of the flame. The time separation between images is 75 ms. In the PIV image a mean vertical velocity of 24 m/s has been subtracted from the velocity vectors.
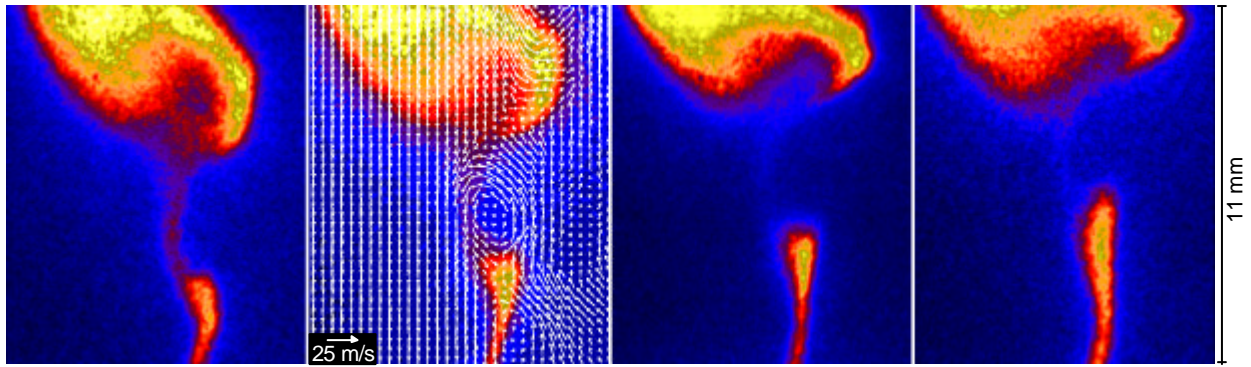
Figure 5: A local extinction phenomenon at a position around 80 mm above the burner, the time separation between images is 75 μs. In the PIV image a mean vertical velocity of 19 m/s has been subtracted from the velocity vectors.

The time development of the OH distribution and the corresponding velocity field near a region of local OH extinction in the lower part of the flame is shown in figure 4. The imaged region corresponds to 8x12 mm, starting 14 mm over the burner nozzle, the time separation between the OH PLIF images is 75 μs. The vortex in the upper part of the image impinges on the flame front, forces it to bulge slightly outwards, and finally quenches the flame locally, leaving a gap in the flame front.

This phenomenon was also observed by (Takahashi et al., 1996) who found that local extinction in a similar flame was primarily caused by the unsteady radial movement of internal vortices which rapidly passed through the flame zone. According to (Takahashi and Katta, 1996 and Katta et al., 1998) the local extinction caused by the internal vortices is largely due to unsteady transport effects on chemical kinetics. When the vortex approaches the flame front it strains the front and the steep fuel concentration gradient ahead of its leading edge causes a large fuel flux into the reaction zone. This large flux of methane and also of some preformed methyl radicals into the reaction zone depletes the radical pool (OH, H and O) in the strained flame zone, and thus quenches the flame locally.

In the velocity field several small vortices are seen rolling up along the flame front on the fuel side (right side). These are axi-symmetric vortices which evolve along the shear layer between the fuel and air flows, the rotational axis of the vortices is parallel to the flame front and oriented horizontally.

In figure 5 a local extinction event caused by a large vortex penetrating the flame front is shown. The imaged region corresponds to 11x13 mm, starting 75 mm above the burner nozzle, the time separation between the OH PLIF images is 75 μs. In the sequence a large vortex extinguishes the flame front just below a thickened OH region. In the first frame an already thinned and weakened flame front is seen, in the next frame the vortex structure is actually seen inside the opening flame front gap, as it is in the process of penetrating through it. At this height in the flame the vortices have grown in size and turbulence has spread into the core of the fuel flow.

In figure 6 a local extinction event in the upper part of the flame is shown. The imaged region corresponds to 14x16 mm, starting 144 mm over the burner nozzle, the time separation between the OH PLIF images is 125 μs.
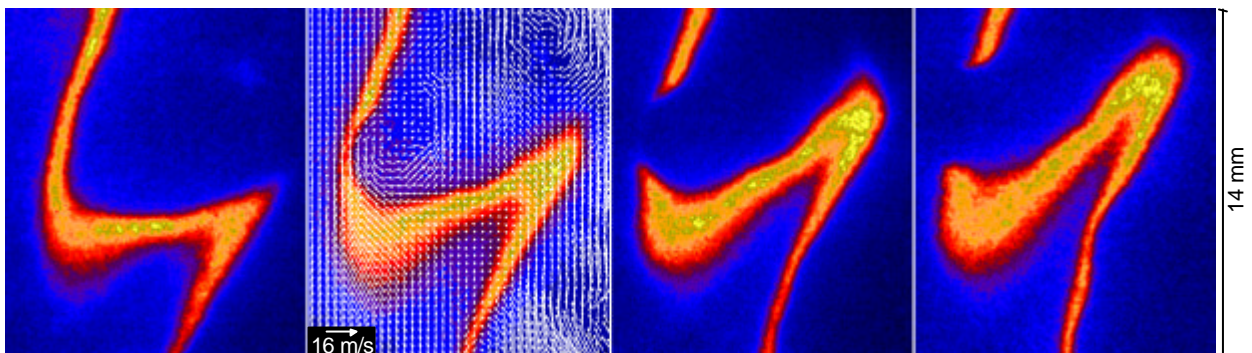

Figure 6: A local extinction phenomenon at a position around 150 mm above the burner, the time separation between images is 125 μs. In the PIV image a mean vertical velocity of 9 m/s has been subtracted from the velocity vectors.

In the second image a vortex is seen, approaching the flame front and forcing it to bulge out slightly, a decrease in the OH concentration can also be seen at the top of the bulge. In the next frame the flame has just extinguished as indicated by the sharpness of the two tips of the now separated flame fronts. The large scale wrinkling of the flame front in this downstream part of the flame is clearly seen. Three relatively large regions with high and uniformly directed velocities act to twist the already s-shaped flame front even further, they are seen to the lower left, lower right and center right part, respectively, of the flow field image.
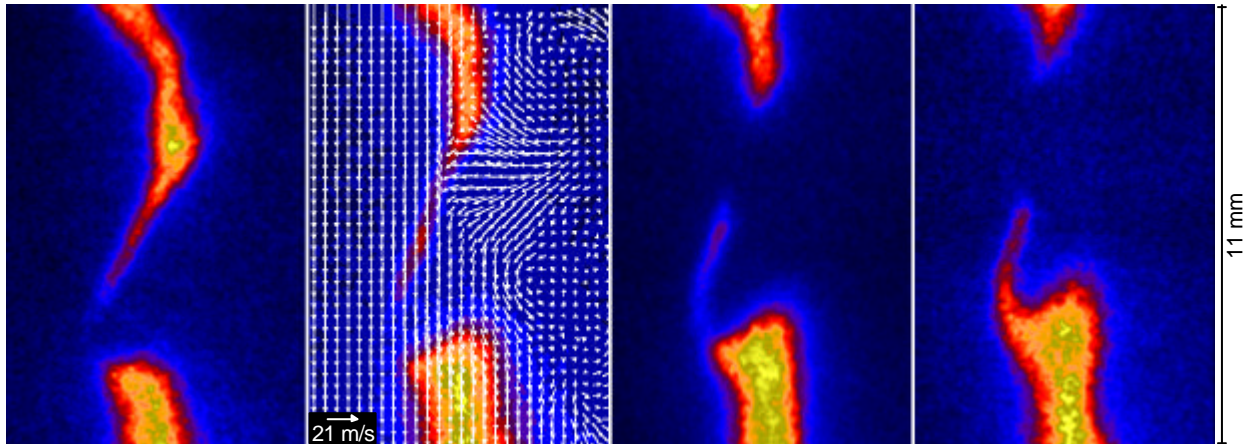

Figure 7: A local extinction phenomenon at a position around 45 mm above the burner, the time separation between images is 75 μs. In the PIV image a mean vertical velocity of 24 m/s has been subtracted from the velocity vectors.

In figure 7 the local extinction event is caused by a flow structure with a different orientation than the vortices seen in the previous images. The imaged regions corresponds to 8x11 mm, starting 38 mm over the burner nozzle, the time separation between the OH PLIF images is 75 μs. The structure is either a jet of fuel impinging on the flame front, or a vortex (of which only one half is seen) with a vertically oriented rotational axis. The rotational axis of the vortices formed at the base of the flame all have the same direction, as they are transported further up in the flow the direction of the rotational axis may change.

From the OH PLIF sequences covering individual extinction events the time scale of these events can be estimated. Judging from the sequences recorded in this study the extinction of the flame front seems to occur on a time scale faster than or on the same order of magnitude as the time separation between consecutive images, thus establishing an upper limit for extinction events of about 100 μs.

In figure 8 re-ignition of a locally extinguished flame front is seen. The imaged region corresponds to 11x14 mm, starting 121 mm over the burner nozzle, the time separation between the OH PLIF images is 125 μs. An
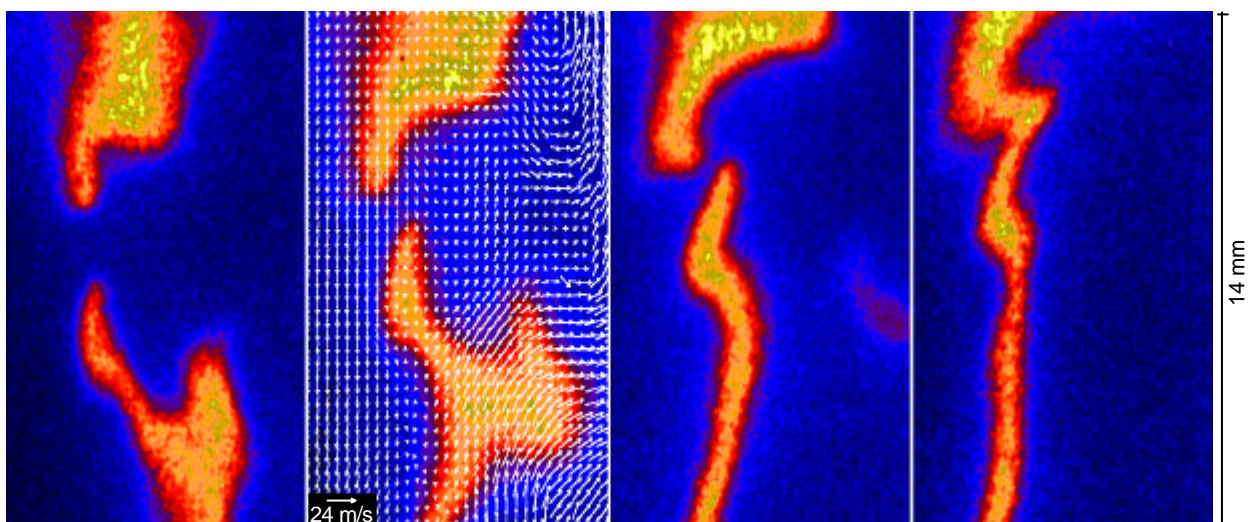

Figure 8: Re-ignition of a gap in the flame front, the time separation between images is 125 μs. In the PIV image a mean vertical velocity of 13.5 m/s has been subtracted from the velocity vectors.

7

extinguished flame region can re-ignite first when an ignitable mixture of fuel and air has been established again and reached ignition temperatures. In the image sequence the gradual re-ignition of the region separating the two flame front tips is seen. The corresponding velocity field indicates that the re-ignition takes place in a region of relatively homogeneous flow.

4. CONCLUSIONS

The present study reports on the first sequentially time resolved OH PLIF and instantaneous PIV measurements of flame extinction in a turbulent flame environment. The technique was demonstrated in the TECFLAM turbulent non-premixed jet flame in an effort to increase the knowledge base existing for this flame which acts as a reference for model development and validation. In the high repetition rate OH PLIF sequences the response of the reaction zone to various structures in the turbulent flow could be studied and the starting point of local extinction events could be located in both space and time. The flow field structures associated with the identified extinction events were captured by the simultaneous PIV measurements. The sequences illustrated that local extinction of this flame was mainly caused by vortices impinging from the fuel side onto the reaction zone. In the lower part of the flame all vortices had the same rotational direction, and only higher up had the structures become sufficiently randomized for other rotational directions to appear responsible for extinction events. From the sequences the maximum time scale of the extinction events was estimated to 100 µs. An example of flame re-ignition in a region of relatively homogeneous flow was also shown.

The extinction sequences presented in this study are part of an extensive data set, which will be analyzed statistically. For example the strain rate limit above which extinction is likely to occur can be established. A possibility the presented technique may offer is to make possible the separation of the effects of flow and chemistry on the local flame front structure. From the OH PLIF sequences the velocity of the flame front movement can be extracted, which is a function of both global flow and chemistry effects. The combined PIV measurement, giving flow velocity alone, may thus allow the chemistry part to be isolated.

The use of time resolved OH PLIF to locate extinction events can be combined with various other measurement techniques in addition to PIV to study additional flame quantities, giving further insight into the details of local extinction.

REFERENCES

Aldén, M., Edner, H., Holmstedt, G., Svanberg, S. and Högberg, T. (1982). "Single-pulse laser-induced OH fluorescence in an atmospheric flame, spatially resolved with a diode array detector", Appl. Optics, vol. 21, pp. 1236-1240

Bergmann, V., Meier, W., Wolff, D. and Stricker, W. (1998). "Application of spontaneous Raman and Rayleigh scattering and 2D LIF for the characterization of a turbulent $CH_4/H_2/N_2$ jet diffusion flame", Appl. Phys. B, vol. 66, pp. 489-502

Cuenot, B. and Poinsot, T. (1994) "Effects of curvature and unsteadiness in diffusion flames, implications for turbulent diffusion flames", Proc. Comb. Inst. 25, The Combustion Institute, Pittsburgh, pp. 1383-1390

Dantec Measurement Technology (1997). "FlowMap Installation & User's guide"

Ding, T., van der Meer, Th., Versluis, M., Golombok, M., Hult, J., Aldén, M. and Kaminski, C.F. (2000). "Time-resolved PLIF imaging in turbulent diffusion flames", Proc. 3rd Int. Symp. On Turbulence, Heat, and Mass Transfer, Nagoya, pp. 857-864

Engström, J., Kaminski, C.F., Aldén, M., Josefsson, G. and Magnusson, I. (1999) "Experimental investigations of flow and temperature fields in an SI engine and comparison with numerical analysis", SAE Paper 1999-01-3541

Hanson, R.K. (1986). "Combustion Diagnostics: Planar Imaging Techniques", Proc. Comb. Inst. 21, The Combustion Institute, Pittsburgh, pp. 1677-1691

Kaminski, C.F., Hult, J. and Aldén, M. (1999). "High repetition rate planar laser induced fluorescence of OH in a turbulent non-premixed flame", Appl. Phys. B, 68, pp. 757-760

Katta, V.R., Hsu, K.Y. and Roquemore, W.M. (1998) "Local extinction in an unsteady methane-air jet diffusion flame", Proc. Comb. Inst. 27, The Combustion Institute, Pittsburgh, pp. 1121-1129

Klingmann, J., Johansson, B. and Josefsson, G. (1997) "Laminar and turbulent flame velocity measurements in a lean stationary premixed methane/air flame", 7th International Conference Laser Anemometry Advances and Applications, Karlsruhe

Kychakoff, G., Paul, P.H., van Cruynigen, I. and Hanson R.K. (1987). "Movies and 3-D images of flowfields using planar laser-induced fluorescence", Appl. Opt., vol. 26, pp. 2498-2500

Oakley, T.R., Loth, E. and Adrian, R.J. (1996) "Cinematic particle image velocimetry of high-Reynolds-number turbulent free shear layer", AIAA Journal, vol. 34, pp. 299-308

Raffel, M., Willert, C. and Kompenhaus, J. (1998) "Particle Image Velocimetry", Springer Verlag, Berlin

Rehm, J.E. and Clemens, N.T. (1998). "The relationship between vorticity/strain and reaction zone structure in turbulent non-premixed jet flames", Proc. Comb. Inst. 27, The Combustion Institute, Pittsburgh, pp. 1113-1120

Schefer, R.W., Namazian, M., Filtopoulos, E.E.J. and Kelly, J. (1994) "Temporal evolution of turbulence/chemistry interactions in lifted, turbulent-jet flames", Proc. Comb. Inst. 25, The Combustion Institute, Pittsburgh, pp. 1223-1231

Seizmann, J.M., Miller, M.F., Island, T.C. and Hanson, R.K. (1994). "Double pulse imaging using simultaneous OH/acetone PLIF for studying the evolution of high speed reacting mixing layers", Proc. Comb. Inst. 25, The Combustion Institute, Pittsburgh, pp. 1743-1750

Sonka, M., Hlavac, V. and Boyle R. (1993) "Image Processing, Analysis and Machine Vision", Chapman&Hall, London

Stårner, S.H., Bilger, R.W., Dibble, R.W., Barlow, R.S., Fourguette, D.C. and Long M.B. (1992) "Joint planar CH and OH LIF imaging in piloted turbulent jet diffusion flames near extinction", Proc. Comb. Inst. 24, The Combustion Institute, Pittsburgh, pp. 341-349

Takahashi, F. and Goss, L.P. (1992) "Near-field turbulent structures and the local extinction of jet diffusion flames", Proc. Comb. Inst. 24, The Combustion Institute, Pittsburgh, pp. 351-359

Takahashi, F., Schmoll, W.J., Trump, D.D. and Goss, L.P. (1996) "Vortex-flame interactions and extinction in turbulent jet diffusion flames", Proc. Comb. Inst. 26, The Combustion Institute, Pittsburgh, pp. 145-152

Takahashi, F. and Katta, V.R. (1996) "Unsteady extinction mechanisms of diffusion flames", Proc. Comb. Inst. 26, The Combustion Institute, Pittsburgh, pp. 1151-1160

Watson, K.A., Lyons, K.M., Donbar, J.M. and Carter, C.D. (1999). "Scalar and Velocity Field in a Lifted CH_4-Air Diffusion Flame", Combust. and Flame, vol. 117, pp. 257-271